Processing of Electroactive Nanostructured Films Incorporating Carbon Nanotubes and Phthalocyanines for Sensing

ARTICLE *in* THE JOURNAL OF PHYSICAL CHEMISTRY C · MAY 2008

Impact Factor: 4.77 · DOI: 10.1021/jp800976f

Processing of Electroactive Nanostructured Films Incorporating Carbon Nanotubes and Phthalocyanines for Sensing

José R. Siqueira, Jr.,[†] Luiz H. S. Gasparotto,[‡] Osvaldo N. Oliveira, Jr.,[†] and Valtencir Zucolotto*,[†]

Universidade de São Paulo, IFSC, CP 369, São Carlos, SP, 13560-970, Brazil, and Universidade Federal de São Carlos, DQ, CP 676, São Carlos, SP, 13565-905, Brazil

Received: February 1, 2008; Revised Manuscript Received: March 13, 2008

The use of carbon nanotubes (CNTs) combined with other materials in nanostructured films has demonstrated their versatility in tailoring specific properties. In this study, we produced layer-by-layer (LbL) films of polyamidoamine-PAMAM-incorporating multiwalled carbon nanotubes (PAMAM-NT) alternated with nickel tetrasulfonated metallophthalocyanine (NiTsPc), in which the incorporation of CNTs enhanced the NiTsPc redox process and its electrocatalytic properties for detecting dopamine. Film growth was monitored by UV−vis spectroscopy, which pointed to an exponential growth of the multilayers, whose roughness increased with the number of bilayers according to atomic force microscopy (AFM) analysis. Strong interactions between $-NH_3^+$ terminal groups from PAMAM and $-SO_3^-$ from NiTsPc were observed via infrared spectroscopy, while the micro-Raman spectra confirmed the adsorption of carbon nanotubes (CNTs) onto the LbL film containing NiTsPc. Cyclic voltammograms presented well-defined electroactivity with a redox pair at 0.86 and 0.87 V, reversibility, a charge-transfer controlled process, and high stability up to 100 cycles. The films were employed successfully in dopamine (DA) detection, with limits of detection and quantification of 10^{-7} and 10^{-6} mol L^{-1}, respectively. Furthermore, films containing immobilized CNTs could distinguish between DA and its natural interferent, ascorbic acid (AA).

1. Introduction

Nanoscale manipulation has brought tremendous advances in materials science with novel materials being produced with unique properties for applications in optical and electronic devices, and in (bio)sensing.[1–5] Among the most studied materials are carbon nanotubes (CNTs) [6–8] that exhibit unprecedented mechanical strength, in addition to interesting electronic and chemical properties.[9–11] They can be either single-walled (SWNTs) or multiwalled (MWNTs) and may be combined with substances such as polymers[12] and metal nanoparticles.[13] In the latter cases, manipulation of CNTs at the molecular level in ultrathin films may be required.[14–16] In this context, the layer-by-layer (LbL) technique appears as one of the most suitable strategies owing to the possible control of film architecture, in which synergy between distinct materials may be achieved.[1,2,17–19] This method, based on electrostatic interactions of oppositely charged layers, allows the use of a diversity of organic and inorganic substances, including CNTs,[9] proteins,[20] antigen−antibody pairs,[21] DNA,[22] nanoparticles,[23] metallophthalocyanines,[24] and dendrimers.[25]

The properties of LbL films of a given material depend largely on the accompanying materials employed, which allows a fine-tuning of specific, desired properties. In this study, we combine CNTs with metallophthalocyanines (MPc), coordination compounds with well-defined redox activities and electrocatalysis abilities,[26–29] and polyamidoamine (PAMAM) dendrimers that are highly branched polymers. Unlike classical polymers, dendrimers have a narrow molecular weight distribution, characteristic size and shape, and a highly functionalized terminal surface.[30] In the LbL films, PAMAMs have been used as polycationic compounds [21,23,25] because of their high density of active groups and biocompatibility. We present a new LbL nanostructured electroactive film based on tetrasulfonated metallophthalocyanine of nickel (NiTsPc) and PAMAM dendrimers incorporating multiwalled carbon nanotubes (MWNTs). The physicochemical and electrochemical properties of the LbL films are analyzed, as well as their capability to detect dopamine in the presence of a possible interferent (ascorbic acid).

2. Experimental Section

2.1. Reagents and Solutions. Ni(II)TsPc, G4 PAMAM dendrimer, and multiwalled carbon nanotubes (MWNTs) were purchased from Aldrich Co. The aqueous solutions of NiTsPc and PAMAM were used at concentrations of 0.5 and 1.0 g L^{-1}, respectively. Both solutions were prepared at pH 4 and room temperature. The PAMAM-NT solution was prepared by adding 10 mg of purified MWNTs in 10 mL of PAMAM solution under utrasonication for 2 h, followed by filtration. The pH of the PAMAM-NT solution was adjusted to 4 using a 1.0×10^{-1} mol L^{-1} H_2SO_4 solution. Dopamine (DA) (3-Hydroxytyramine hydrochloride, $C_8H_{11}NO_2 \cdot HCl$) was purchased from Fluka and used at concentrations from 1.0×10^{-5} to 1.0×10^{-3} mol L^{-1}, prepared in 1.0×10^{-1} mol L^{-1} H_2SO_4 solution. Ascorbic acid (AA) ($C_6H_8O_6$) was purchased from Merck and used at concentration of 5.0×10^{-3} mol L^{-1}, being prepared in the same H_2SO_4 solution used for DA.

2.2. MWNT Purification. The MWNTs were purified according to the following procedure: 100 mg of MWNTs was oxidized at 400 °C for 45 min to remove amorphous carbon particles. The oxidized CNTs were dispersed in 60 mL of 6.0

* Corresponding author. Address: Instituto de Física de São Carlos, Universidade de São Paulo. Av. Trabalhador Sãocarlense, 400, P.B. 369, Zip: 13560-970, São Carlos - SP - Brazil. Phone: +55 16 3373 9825; fax: +55 16 3371 5365; e-mail: zuco@ifsc.usp.br.

[†] Universidade de São Paulo.

[‡] Universidade Federal de São Carlos.

10.1021/jp800976f CCC: $40.75
Published on Web 05/28/2008

mol·L^{-1} HCl solution for 4 h under ultrasonic stirring to eliminate metal oxide catalysts and washed thoroughly with Mili-Q water under centrifugation to remove any remaining acid until the pH of the solution was neutral, followed by drying in an oven at 60 °C.

2.3. LbL Film Fabrication. PAMAM/NiTsPc and PAMAM-NT/NiTsPc LbL films containing 1, 3, 5, 10, and 15 bilayers were fabricated by immersing the substrates alternately into the polycationic PAMAM (5 min) or PAMAM-NT (10 min) and anionic NiTsPc (5 min) solutions. After deposition of each layer, the films were rinsed in a washing solution at pH 4 and dried under a N_2 flow. The schematic representation of a one-bilayer PAMAM-NT/NiTsPc LbL film and the chemical structures of the materials employed can be seen in the Supporting Information.

2.4. Characterization. The multilayer growth was monitored by measuring the UV−vis spectra up to the 10th bilayer deposited on a glass substrate coated with an indium−tin-oxide (ITO) film, using a Hitachi U-2001 spectrophotometer. Fourier transform infrared spectroscopy (FTIR) experiments were carried out in 15-bilayer LbL films deposited on silicon substrates for the transmission mode, using a Nicolet 470 Nexus spectrometer. Neat NiTsPc, PAMAM, and PAMAM-NT were analyzed as cast films. The Raman spectra were recorded using a micro-Raman spectrograph Renishaw Research Raman Microscope System RM2000 recorded with the 633 nm laser line. The equipment contains a Leica Microscope (DMLM series) and a 50x-microscope objective to focus the laser beam onto a spot of ca. 1.0 μm^2. The film morphology was studied in LbL films containing 1, 3, 5, and 10 bilayers deposited onto ITO-coated glass substrates, using an atomic force microscope (AFM) Nanoscope III (Digital Instruments). Cyclic voltammograms were taken with an EG&G PAR M280 potentiostat using LbL films with 1, 3, 5, and 10 bilayers on ITO-coated glass as the working electrode ($A = 0.4$ cm^2). An Ag/AgCl electrode was used as the reference electrode, and a 1.0 cm^2 platinum foil was employed as the counter-electrode. The electrochemical measurements were carried out at room temperature and various scan rates (10, 30, 50, 75, and 100 mV s^{-1}) using a 0.1 mol L^{-1} H_2SO_4 solution as the support electrolyte. Before each measurement, N_2 was bubbled in the electrolytic solution to eliminate dissolved O_2.

2.5. Dopamine Detection. Both film architectures (PAMAM/NiTsPc and PAMAM-NT/NiTsPc) were tested for evaluating their catalytic properties in the presence of a DA solution that ranged from 2.5×10^{-6} to 2.4×10^{-4} mol L^{-1} at 50 mV s^{-1}. The ability of the CNT-incorporated films to distinguish between DA and AA was performed via cyclic voltammetry using an electrolytic solution containing both AA and DA (at various concentrations). In order to simultaneously evaluate the influence of DA concentration and number of bilayers (independent variables) on the DA response, we used a 2^2 full factorial design (its parameters are depicted in the Supporting Information) to investigate the PAMAM-NT/NiTsPc system. The data were fitted as first-order equations with the software STATISTICA to generate the response surfaces.

3. Results and Discussion

3.1. Spectroscopy and Microscopy Characterization of the Films. UV−vis spectra for NiTsPc aqueous solution and 10-bilayer films of PAMAM/NiTsPc and PAMAM-NT/NiTsPc are shown in Figure 1. The intense band between 600 and 700 nm is assigned to absorption of the NiTsPc Q-band.[26] For the NiTsPc solution, there is a shoulder at 660 nm related to monomeric species and an intense absorbance at 625 nm,

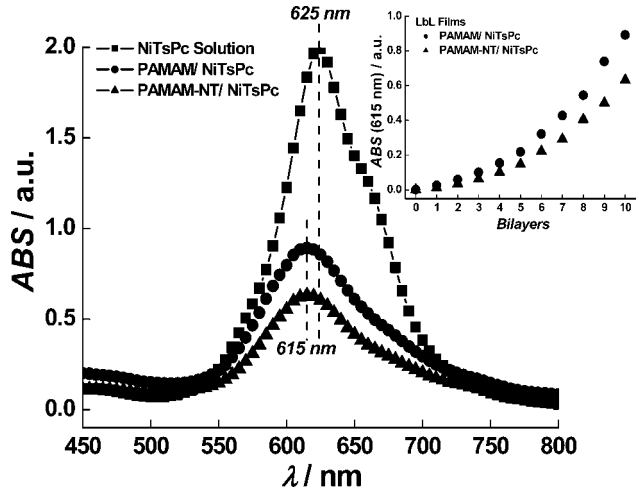

Figure 1. Electronic spectra for NiTsPc aqueous solution and 10-bilayer LbL films of PAMAM/NiTsPc and PAMAM-NT/NiTsPc. Inset: Exponential growth for 10-bilayer LbL films of PAMAM/NiTsPc and PAMAM-NT/NiTsPc.

characteristic of dimeric species.[26] In contrast, for the LbL films the band at 660 nm is not observed, suggesting that NiTsPc are aggregated mainly in dimeric form. A blue shift (ca. 5 nm) is observed in the spectra of the films, in comparison to the NiTsPc solution, which is probably due to H-aggregate formation and may be indicative of interactions among the materials or aggregation of NiTsPc molecules.[28] The inset of Figure 1 shows the film growth, where the amount of adsorbed material, taken as proportional to the absorption at 615 nm, increases exponentially. The latter findings are similar to previous work reported with LbL films of PAMAM-incorporating Pt-nanoparticles/NiTsPc,[29] although it is in contrast to the linear increase reported by Zucolotto et al. and Siqueira Jr. et al. for LbL films of polyaniline/NiTsPc[27] and chitosan/NiTsPc.[28] This exponential growth may result from polyelectrolytes diffusing into the film during its fabrication, as proposed by Picart et al. [31] and Garz et al.[32] Moreover, the stronger adsorption of PAMAM/NiTsPc LbL films in comparison to PAMAM-NT/NiTsPc LbL films for the same number of bilayers might be attributed to the presence of CNTs hampering adsorption of NiTsPc.

The growth and formation of PAMAM/NiTsPc and PAMAM-NT/NiTsPc LbL films were also analyzed by AFM images at a scanned area of 1.0×1.0 μm^2 as shown in Figure 2. Both architectures showed a well-defined film formation because the deposition of the first bilayer and their thicknesses were similar. The roughness (rms) of the PAMAM-NT/NiTsPc LbL film was almost 3 times higher, indicating that CNTs dispersed in PAMAM affect the LbL film formation and morphology directly. The AFM images showed that both roughness and thickness increased with the number of bilayers for PAMAM/NiTsPc and PAMAM-NT/NiTsPc, especially for the latter system as shown in Table 1. Furthermore, after five bilayers of PAMAM-NT/NiTsPc, the structures coalesced and formed large globular islands whose peaks reached ca. 80−120 nm.

Figure 3a shows FTIR spectra for 15-bilayer PAMAM/NiTsPc and PAMAM-NT/NiTsPc LbL films and for neat PAMAM, PAMAM-NT and NiTsPc cast films. PAMAM and PAMAM-NT spectra contain two bands, at 1663 and 1553 cm^{-1}, assigned to the amide band I (C═O stretching) and amide band II (C−N bending) from PAMAM, respectively.[33] These bands were also present in the LbL films, confirming dendrimer

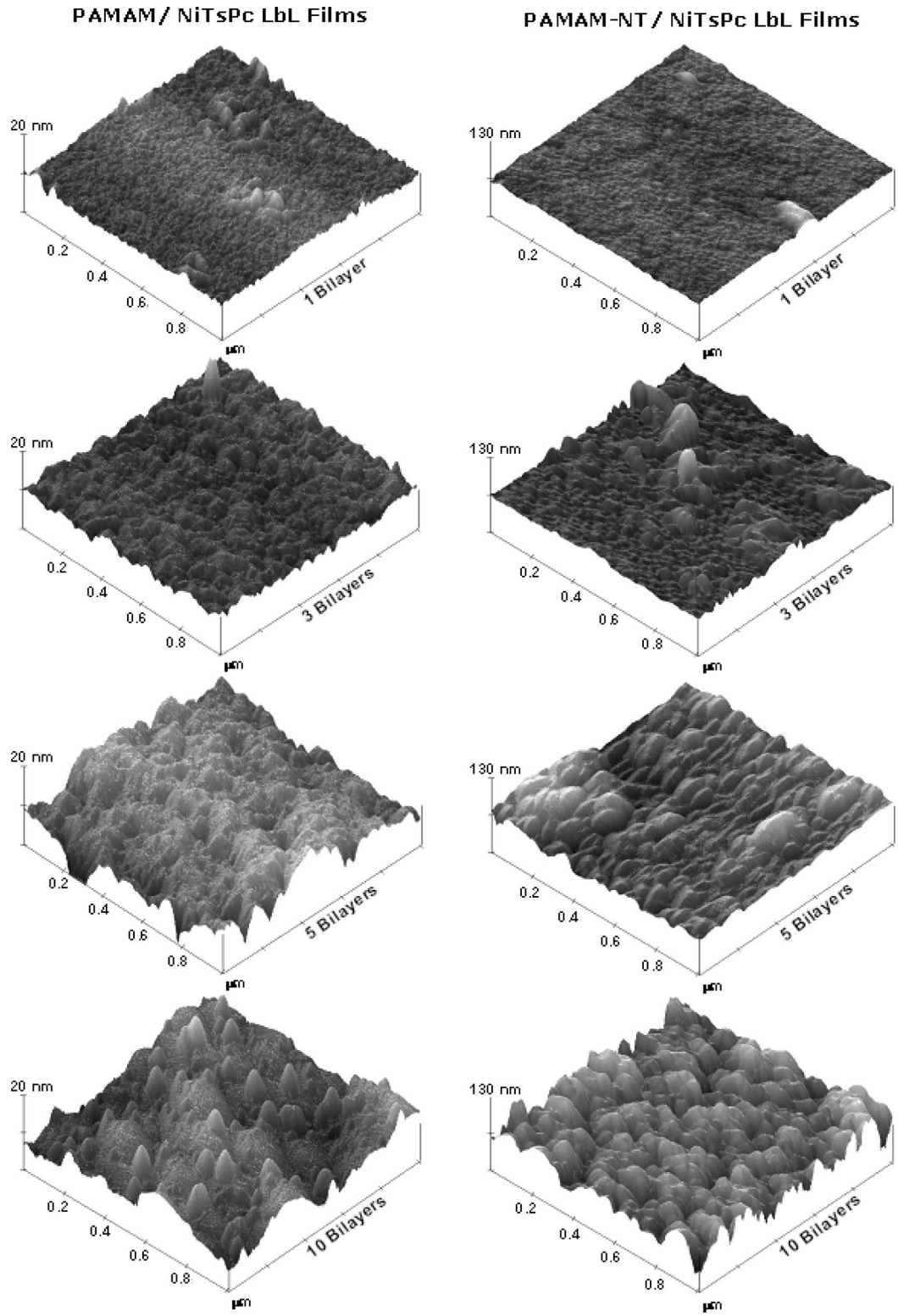

Figure 2. AFM images for LbL films with different numbers of bilayers of PAMAM/NiTsPc and PAMAM-NT/NiTsPc. Note the difference in the scale of the *Z* axis for CNT-containing systems.

incorporation into the film. The band at 1089 cm^{-1} in the PAMAM spectrum, assigned to C−N stretching,[33] was shifted to 1104 cm^{-1} in the PAMAM-NT spectrum, which may be related to a change in orientation of the C−N vibration modes due to the presence of CNTs. The PAMAM spectrum also displays a band assigned to the N−C═O bend (at 622 cm^{-1}), which was not observed in the PAMAM-NT spectrum because it was masked by the more intense band at 610 cm^{-1} associated with the C−C vibration,[34] thus indicating immobilized CNTs in the dendrimer. The NiTsPc spectrum showed bands at 1194 and 1041 cm^{-1}, assigned to SO_3^- stretching, which shifted to 1173 and 1024 cm^{-1} when compared to PAMAM/NiTsPc and PAMAM-NT/NiTsPc LbL films' spectra. In agreement with previous reports (refs 24 and 28), the shifts are due to the electrostatic interaction between the SO_3^- groups of the NiTsPc with NH_3^+ groups of PAMAM. Moreover, a new band (not observed in the NiTsPc spectrum) arose in the spectra of the LbL films at 1059 cm^{-1}, which corresponds to the C−N

TABLE 1: Thickness and Roughness Exhibited by the LbL Fims Employed

	number of bilayers	thickness (nm)	rms roughness (nm)
PAMAM/ NiTsPc	1	1.46	1.65
	3	6.21	2.11
	5	8.84	4.49
	10	72.22	5.27
PAMAM-NT/ NiTsPc	1	1.55	4.12
	3	35.04	16.21
	5	35.52	16.77
	10	100.83	27.67

stretching of PAMAM. These interactions may be associated with the intimate contact between the components of the LbL architecture.

Micro-Raman experiments were carried out for neat CNT and NiTsPc powders, PAMAM-NT cast film, and LbL films containing 10 bilayers of PAMAM-NT/PSS (PSS = sulfonated polystyrene) coated by one-bilayer PAMAM-NT/NiTsPc. The results are shown in Figure 3b. The CNT spectrum presented two bands at 1600 and 1335 cm^{-1}, assigned to G and D bands, respectively.[35] For PAMAM-NT, the G band was shifted to 1592 cm^{-1}, which may be related to the PAMAM molecules attached to the CNT surface, while the D band practically disappeared. Because the D band is assigned to amorphous carbon and impurities,[35–37] the spectrum indicates a high-purity degree of CNTs in PAMAM solution after the purification process.[36,37] The adsorption of CNTs in the PAMAM-NT/NiTsPc LbL film was not apparent (not shown) in the Raman spectrum because the higher amount of NiTsPc adsorbed onto the LbL film generated an intense signal at 1554 and 1337 cm^{-1} (both assigned to pyrrole stretching). Therefore, in order to show the CNT adsorption, we prepared a 10-bilayer PAMAM-NT/PSS LbL film, onto which a NiTsPc layer was deposited. It was then possible to distinguish the bands assigned to CNT (G band at 1592 cm^{-1}) and NiTsPc (pyrrole stretching at 1556 cm^{-1}) in the Raman spectrum.

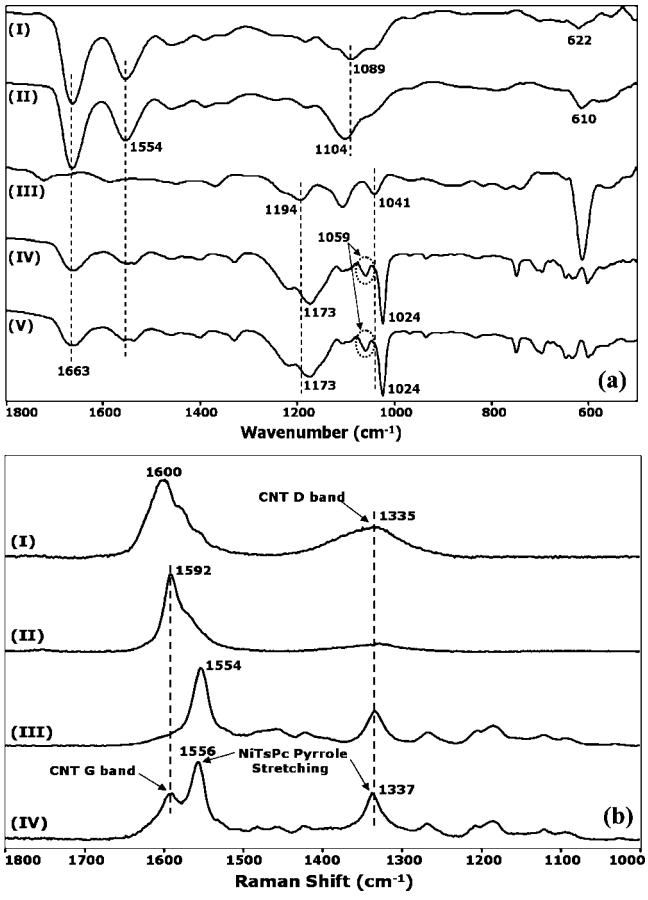

Figure 3. FTIR spectra in transmission mode for cast films of PAMAM (I), PAMAM-NT (II), NiTsPc (III), and 15-bilayer LbL films of PAMAM/NiTsPc (IV) and PAMAM-NT/NiTsPc (V) (a). Raman spectra recorded with a 633-nm laser line for neat CNTs powder (I), PAMAM-NT cast film (II), neat NiTsPc powder (III), and a 10-bilayer LbL film of PAMAM-NT/ PSS + one-bilayer LbL film of PAMAM-NT/NiTsPc (IV) (b).

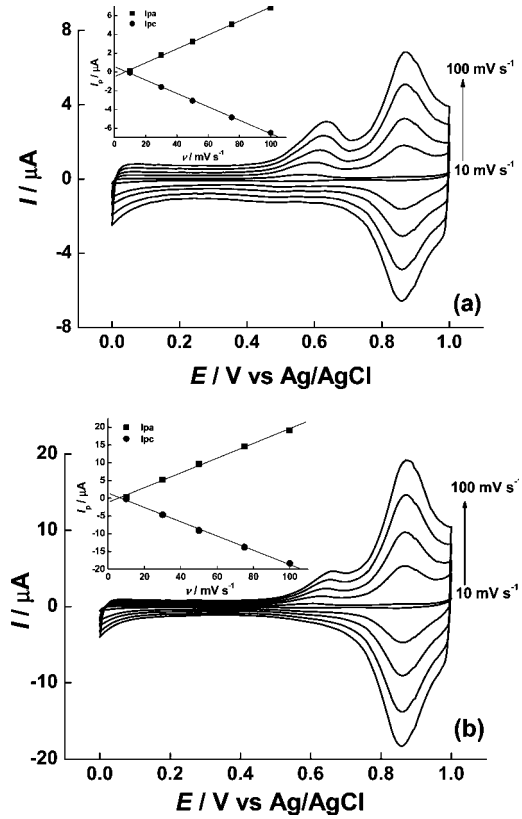

Figure 4. Cyclic voltammograms for three-bilayer LbL films of PAMAM/NiTsPc (a) and PAMAM-NT/NiTsPc (b) at various scan rates. Insets: Linear relationship between anodic and cathodic peak currents and scan rate.

3.2. Electrochemical Characterization of LbL Films. Figure 4 shows cyclic voltammograms for a three-bilayer LbL film of PAMAM/NiTsPc (a) and PAMAM-NT/NiTsPc (b) at various scan rates. Both electrodes exhibited well-defined electroactivity and the same redox pair at 0.86 and 0.87 V, which is attributed to the electrochemical conversion of the NiTsPc *Pc* unit [Ni(II)TsPc^{4-}/Ni(II)TsPc^{6-}].[38] The same redox process has been observed for chitosan/NiTsPc LbL films.[28] The inset of Figure 4 shows that the anodic and cathodic peak currents (I_{pa} and I_{pc}) increased linearly with the scan rate, indicating a charge-transfer-controlled process.[39] Furthermore, the redox peak potentials were the same at different scan rates for both electrodes; the difference between the anodic and cathodic potential peaks is only 10 mV, and the ratio between anodic and cathodic peak current is 1.0, which indicates the reversible character of these films.[40] The anodic peak around 0.6 V may be related to the irreversible [Ni(II)TsPc^{6-}/Ni(II)TsPc^{5-}] process[38] because the peak shifted with the scan rate and its cathodic counterpart was absent. This process was not observed in our previous study on chitosan-metallophthalocyanines nanocomposites,[28] which is indicative

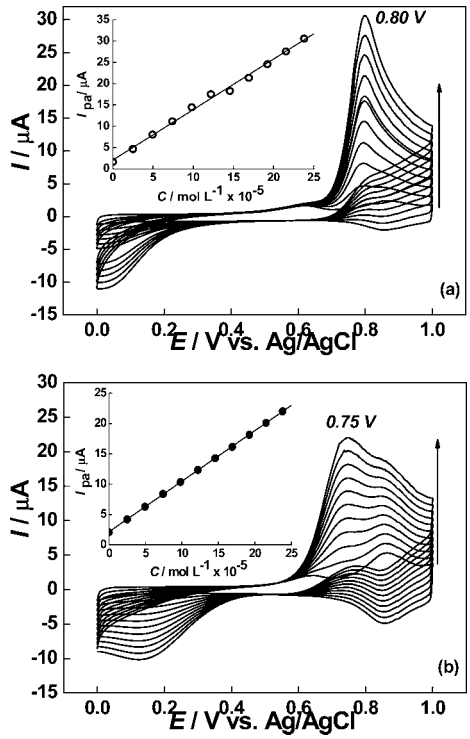

Figure 5. Cyclic voltammograms for three-bilayer LbL films of PAMAM/NiTsPc (a) and PAMAM-NT/NiTsPc (b) at various DA concentrations. Insets: Linear calibration curves. Scan rate: 50 mV s^{-1}.

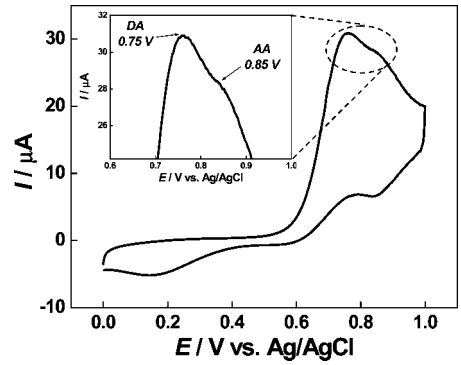

Figure 6. Cyclic voltammograms for simultaneous detection of DA and AA at the same proportion (2.4×10^{-4} mol L^{-1}) for 3-bilayer PAMAM-NT/NiTsPc LbL films. Scan rate: 50 mV s^{-1}.

TABLE 2: Peak Current Potential (E_{pa}) for PAMAM/ NiTsPc and PAMAM-NT/NiTsPc LbL Films in the Presence of DA and AA

	DA detection - E_{pa} (V)	AA detection - E_{pa} (V)
PAMAM/ NiTsPc	0.80	0.85
PAMAM-NT/ NiTsPc	0.75	0.85

that PAMAM did not hamper the NiTsPc charge-transfer process. The electrochemical behavior of NiTsPc in solution is completely different from that in LbL films. All of the processes are irreversible and appear at more positive potentials (not shown). This is evidence that the nanostructured nature of the LbL films may facilitate charge transfer for NiTsPc films. The advantages of the LbL technique was further confirmed upon using cast or spin-coated films containing the same three components, that is, PAMAM, CNTs and NiTsPc. The latter films were not stable, presenting a considerable loss of material during the electrochemical experiments.

Also important to note is that films containing CNTs (Figure 4b) displayed redox currents ca. 3 times higher than films containing only the NiTsPc (Figure 4a). This significant increase in the current values may be explained by either the larger active area (revealed by the higher roughness) or the higher electrical conductivity of the PAMAM-NT/NiTsPc films. Moreover, stability measurements (100-cycle cyclic voltammograms at 50 mV s^{-1}) were also carried out for five-bilayer PAMAM/NiTsPc and PAMAM-NT/NiTsPc LbL films (not shown). Both films showed high stability when submitted to several cycles and there was no change in the peak current, preserving the voltammetric shape.

3.3. Electrocatalytic Properties of LbL films toward Dopamine (DA). The LbL films were tested as sensor elements for compounds of biological interest. Figure 5 depicts the cyclic voltammograms of three-bilayer LbL films of PAMAM/NiTsPc (a) and PAMAM-NT/NiTsPc (b) at DA concentrations ranging from 2.5×10^{-6} to 2.4×10^{-4} mol L^{-1}. In PAMAM/NiTsPc films, only one redox pair appeared, attributed to a two-electron oxidation/reduction process, where dopamine is oxidized to dopaminequinone.[41] Alternatively, PAMAM-NT/NiTsPc films exhibited two anodic peaks that increased with the concentration and the scan rate, suggesting that the two-electron DA oxidation process occurs separately. For the PAMAM/NiTsPc film, the DA irreversible redox process occurred at 0.03 and 0.80 V, while the same process for PAMAM-NT/ NiTsPc film was shifted to 0.14 and 0.75 V. In other words, the CNTs enhanced the redox process and improved the catalytic properties of NiTsPc, affecting the DA redox process. In both films, the anodic peak current increased linearly with the concentration of DA (as shown in the insets of Figure 5a and b). The latter was important to determine a linear calibration curve to each modified electrode and consequently to calculate the limit of detection (LD) for DA, which was 4.3×10^{-7} and 5.4×10^{-7} mol L^{-1} for PAMAM/NiTsPc and PAMAM-NT/NiTsPc, respectively. These LD values are significantly lower than those reported earlier for LbL film-based systems.[27,28] The limit of quantification (LQ) for DA was also calculated, being 1.4×10^{-6} and 1.8×10^{-6} mol L^{-1} for PAMAM/NiTsPc and PAMAM-NT/NiTsPc, respectively.

In order to investigate the selectivity of the electrodes to DA in the presence of interferent, we added different DA concentrations to a 2.4×10^{-4} mol L^{-1} ascorbic acid (AA) solution. Because the oxidation potential for DA and AA are similar, it was not possible to distinguish the analytes using the PAMAM/ NiTsPc films (not shown). However, PAMAM-NT/NiTsPc films displayed a selective behavior, making it possible to distinguish between the DA (0.75 V) and AA (0.85 V) signals at the same proportion as shown in Figure 6. The selectivity exhibited by the CNTs-containing films is probably related to the electrocalytic effect observed for DA detection in these electrodes (as shown in Figure 5). For clarity, the potentials of the anodic peak current (E_{pa}) for DA and AA for both electrodes are summarized in Table 2.

Because the performance of thin-film-based sensors and biosensors varies considerably with film characteristics, optimized conditions must be investigated. For sensors employing LbL films, this is a time-consuming step because of the large number of variables affecting the film properties. To minimize the analysis time, we used a factorial design,[42] as a proof of concept, to evaluate the influence of the DA concentration and number of bilayers (independent variables) during DA detection. One of the advantages of this method is to obtain valuable

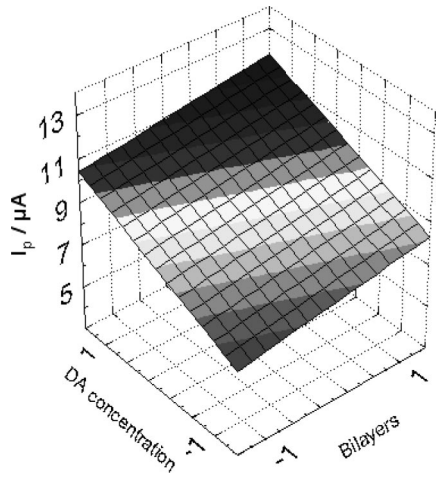

Figure 7. Response surface on dopamine for a PAMAM-NT/NiTsPc LbL film.

information by performing a reduced number of experiments. The parameter taken as indicative of sensitivity was the peak current for the first anodic process of DA oxidation at 10 mV s^{-1}. The results of a 2^2 full factorial design for the PAMAM-NT/NiTsPc system were analyzed by means of the response surface methodology (RSM) as shown in Figure 7.

Both DA concentration and the number of bilayers were found to affect DA detection, but there was no interaction between them because the calculated effect was insignificant. Also, the DA concentration was more significant for DA detection. The number of bilayers also led to a slight enhancement of the DA detection, in terms of peak current, as a result of the increasing surface roughness (see Table 2). However, an increase in the number of bilayers tends to increase the background signal (capacitive current), which is undesirable. In order to reduce the background current and obtain lower detection limits, our recommendation, based on the results of the factorial design, is to use LbL films with only a few bilayers in future sensing applications.

4. Conclusions

The LbL films containing CNTs and NiTsPc studied here exhibited strong interactions, which may be related to the intimate contact between the film components. The incorporation of CNTs in LbL films enhanced the NiTsPc redox process and improved its catalytic activity for dopamine detection, thus leading to modified electrodes with high electroactivity, sensitivity, and selectivity (in the presence of AA). The factorial design suggested the use of few-bilayer LbL films for reducing the background current and leading to lower detection limits.

Acknowledgment. We thank Prof. Edenir Rodrigues Pereira Filho for discussions on the factorial design analysis and Prof. Ricardo Zanatta for the use of the Raman spectroscopy system. Financial support from CAPES, FAPESP, CNPq, and IMMP (Brazil) is gratefully acknowledged.

Supporting Information Available: Schematic representation of a one-bilayer PAMAM-NT/NiTsPc LbL film and the chemical structures of the materials employed, and coded levels and real values for the 2^2 full factorial design. This information is available free of charge via the Internet at http://pubs.acs.org.

References and Notes

(1) Oliveira, O. N., Jr.; Zucolotto, V.; Balasubramanian, S.; Li, L.; Nalwa, H. S.; Kumar, J.; Tripathy, S. K. Layer-by-Layer Polyelectrolyte-Based Thin Films for Electronic and Photonic Applications. In *Handbook of Polyelectrolytes and Their Applications*; Tripathy, S. K., Kumar, J., Nalwa, H. S., Eds.; American Scientific Publishers: Los Angeles, CA, 2002; Vol. *1*, p 1.

(2) Hammond, P. T. *Adv. Mater.* **2004**, *16*, 1271.

(3) Lutkenhaus, J. L.; Hammond, P. T. *Soft Matter* **2007**, *3*, 804.

(4) Ariga, K.; Hill, J. P.; Ji, Q. M. *Phys. Chem. Chem. Phys.* **2007**, *9*, 2319.

(5) Quinn, J. F.; Johnston, A. P. R.; Such, G. K.; Zelikin, A. N.; Caruso, F. *Chem. Soc. Rev.* **2007**, *36*, 707.

(6) Iijima, S. *Nature* **1991**, *354*, 56.

(7) Iijima, S.; Ichihashi, T. *Nature* **1993**, *363*, 603.

(8) Balasubramanian, K.; Burghard, M. *Anal. Bioanal. Chem.* **2006**, *385*, 452.

(9) Olek, M.; Ostrander, J.; Jurga, S.; Mohwald, H.; Kotov, N.; Kempa, K.; Giersig, M. *Nano Lett.* **2004**, *4*, 1889.

(10) Belin, T.; Epron, R. *Mater. Sci. Eng. B* **2005**, *119*, 105.

(11) Thostenson, E. T.; Ren, Z. F.; Chou, T. W. *Compos. Sci. Technol.* **2001**, *61*, 1899.

(12) Yan, Y. M.; Zhang, M. N.; Gong, K. P.; Su, L.; Guo, Z. X.; Mao, L. Q. *Chem. Mater.* **2005**, *17*, 3457.

(13) Yang, M. H.; Yang, Y.; Yang, H. F.; Shen, G. L.; Yu, R. Q. *Biomaterials* **2006**, *27*, 246.

(14) Kim, B.; Sigmund, W. M. *Langmuir* **2004**, *20*, 8239.

(15) Sun, Y. P.; Fu, K. F.; Lin, Y.; Huang, W. J. *Acc. Chem. Res.* **2002**, *35*, 1096.

(16) Chen, J.; Hamon, M. A.; Hu, H.; Chen, Y. S.; Rao, A. M.; Eklund, P. C.; Haddon, R. C. *Science* **1998**, *282*, 95.

(17) Decher, G. *Science* **1997**, *277*, 1232.

(18) Zhao, W.; Xu, J. J.; Chen, H. Y. *Electroanalysis* **2006**, *18*, 1737.

(19) Crespilho, F. N.; Zucolotto, V.; Siqueira, J. R.; Constantino, C. J. L.; Nart, F. C.; Oliveira, O. N., Jr. *Environ. Sci. Technol.* **2005**, *39*, 5385.

(20) Zucolotto, V.; Pinto, A. P. A.; Tumolo, T.; Moraes, M. L.; Baptista, M. S.; Riul, A.; Araujo, A. P. U.; Oliveira, O. N., Jr. *Biosens. Bioelectron.* **2006**, *21*, 1320.

(21) Zucolotto, V.; Daghastanli, K. R. P.; Hayasaka, C. O.; Riul, A.; Ciancaglini, P.; Oliveira, O. N., Jr. *Anal. Chem.* **2007**, *79*, 2163.

(22) Lvov, Y.; Decher, G.; Sukhorukov, G. *Macromolecules* **1993**, *26*, 5396.

(23) Crespilho, F. N.; Huguenin, F.; Zucolotto, V.; Olivi, P.; Nart, F. C.; Oliveira, O. N., Jr. *Electrochem. Commun.* **2006**, *8*, 348.

(24) Zucolotto, V.; Ferreira, M.; Cordeiro, M. R.; Constantino, C. J. L.; Balogh, D. T.; Zanatta, A. R.; Moreira, W. C.; Oliveira, O. N., Jr. *J. Phys. Chem. B* **2003**, *107*, 3733.

(25) Crespilho, F. N.; Zucolotto, V.; Brett, C. M. A.; Oliveira, O. N., Jr.; Nart, F. C. *J. Phys. Chem. B* **2006**, *110*, 17478.

(26) Leznoff, C. C.; Lever, A. B. P. *Phthalocyanines - Properties and Applications*; John Wiley & Sons: New York, 1989; Vol. 3.

(27) Zucolotto, V.; Ferreira, M.; Cordeiro, M. R.; Constantino, C. J. L.; Moreira, W. C.; Oliveira, O. N., Jr. *Sens. Actuators* **2006**, *113*, 809.

(28) Siqueira, J. R.; Gasparotto, L. H. S.; Crespilho, F. N.; Carvalho, A. J. F.; Zucolotto, V.; Oliveira, O. N., Jr. *J. Phys. Chem. B* **2006**, *110*, 22690.

(29) Siqueira, J. R.; Crespilho, F. N.; Zucolotto, V.; Oliveira, O. N., Jr. *Electrochem. Commun.* **2007**, *9*, 2676.

(30) Aulenta, F.; Hayes, W.; Rannard, S. *Eur. Polym. J.* **2003**, *39*, 1741.

(31) Picart, C.; Mutterer, J.; Richert, L.; Luo, Y.; Prestwich, G. D.; Schaaf, P.; Voegel, J. C.; Lavalle, P. *Proc. Natl. Acad. Sci. U.S.A.* **2002**, *99*, 12531.

(32) Garza, J. M.; Schaaf, P.; Muller, S.; Ball, V.; Stoltz, J. F.; Voegel, J. C.; Lavalle, P. *Langmuir* **2004**, *20*, 7298.

(33) Deutsch, D. S.; Siani, A.; Fanson, P. T.; Hirata, H.; Matsumoto, S.; Williams, C. T.; Amiridis, M. D. *J. Phys. Chem. C* **2007**, *111*, 4246.

(34) Pan, B. F.; Cui, D. X.; Gao, F.; He, R. *Nanotechnology* **2006**, *17*, 2483.

(35) Dresselhaus, M. S.; Dresselhaus, G.; Saito, R.; Jorio, A. *Phys. Rep.* **2005**, *409*, 47.

(36) Alvarez, W. E.; Pompeo, F.; Herrera, J. E.; Balzano, L.; Resasco, D. E. *Chem. Mater.* **2002**, *14*, 1853.

(37) Wang, Y. D.; Joshi, P. P.; Hobbs, K. L.; Johnson, M. B.; Schmidtke, D. W. *Langmuir* **2006**, *22*, 9776.

(38) Irvine, J. T. S.; Eggins, B. R.; Grimshaw, J. *J. Electroanal. Chem.* **1989**, *271*, 161.

(39) Laurent, D.; Schlenoff, J. B. *Langmuir* **1997**, *13*, 1552.

(40) Brett, A. M. O.; Brett, C. M. A. *Electroquímica: Princípios, Métodos e Aplicações*; Almedina: Coimbra, 1996.

(41) Lin, X. Q.; Zhang, L. *Anal. Lett.* **2001**, *34*, 1585.

(42) Bruns, R. E.; Scarminio, L. S.; Neto, B. B. *Statistical Design-Chemometrics*; Elsevier: Amsterdam, 2006.

JP800976F